J Mater Sci (2011) 46:6106–6110
DOI 10.1007/s10853-011-5574-9

Preparation of cobalt ferrite nanoparticles by using spent Li-ion batteries

Li Yang · Qinghua Yan · Guoxi Xi · Liyuan Niu · Tianjun Lou · Tianxi Wang · Xinsheng Wang

Received: 13 January 2011 / Accepted: 18 April 2011 / Published online: 3 May 2011

Abstract Cobalt ferrite nanoparticles are a soft magnetic material have been extensively used in many electronic and magnetic applications. In this study, $Co_{0.8}Fe_{2.2}O_4$ nanoparticles with particle size of about 23.5 nm were directly synthesized by sol–gel auto-combustion and calcination methods using spent Li-ion batteries as raw materials. The overall process involves four steps: formation of homogeneous sols; formation of dried gels; combustion of the dried gels; and calcination of the dried gels after combustion at 1173 K for 2 h. The DTA–TG and IR were used to study the auto-combustion and thermal decomposition of the precursor, the morphology and structure of cobalt ferrite nanoparticles were characterized by XRD and TEM techniques. Moreover, the precise metal ion stoichiometry of cobalt ferrite nanoparticles was analyzed by ICP. The results revealed that the auto-combustion process was considered as a heat-induced exothermic oxidation–reduction reaction between nitrate ions and carboxyl group. The XRD patterns of calcination the dried gels after combustion confirmed the single phase spinel structure for the synthesized materials. The crystallite size was calculated from the most intense peak (3 1 1) using the Scherrer equation. The TEM photograph also shown that cobalt ferrite nanoparticles were well-dispersed and with little aggregation.

L. Yang (✉) · L. Niu · T. Lou · T. Wang · X. Wang
Department of Experimental Center, Henan Institute of Science and Technology, Xinxiang 453003, Henan, China
e-mail: manyouhome1998@yahoo.cn

Q. Yan
Department of Life Science and Technology, Xinxiang Medical College, Xinxiang 453003, Henan, China

G. Xi
The Key Laboratory for Environmental Pollution Control of Henan, Chemistry and Environment Science College of Henan Normal University, Xinxiang 453007, Henan, China

Introduction

Nowadays, the usage of Li-ion batteries has rapidly increased because they are widely used as electrochemical power sources in mobile telephones, personal computers, video-cameras, and other modern-life appliances [1]. Li-ion batteries are often superior to conventional systems with aqueous electrolytes such as the nickel–cadmium (Ni–Cd) rechargeable batteries. $LiCoO_2$ is one of the most commonly used materials in Li-ion battery cathodes due to its good performance [2]. The anodic material used in Li-ion batteries is carbon. Li-ion batteries operate by reversible transport from an electrode to another [3]. The charge and discharge processes of batteries with $LiCoO_2$ as a cathode are represented by Eq. 1.

$$LiCoO_2 + 6C \underset{\text{Discharge}}{\overset{\text{Charge}}{\rightleftharpoons}} Li_{(1-x)}CoO_2 + C_6Li_x \qquad (1)$$

Li-ion batteries not only dominate the cellular phones and laptop computer areas, but also will be the first category of dynamic batteries to be chosen to provide power for electronic automobile in the future time. In 2000, the worldwide production of Li-ion batteries reached about 500 millions cells. From this consumption, It is estimated that the amount of spent Li-ion batteries may reach 200–500 tons/year (2002–2006), with significant amounts of cobalt (5–20 wt%) and lithium (2–7 wt%) [4].

$LiCoO_2$, which is used as the cathode material for almost all commercialized Li-ion batteries due to its excellent performances, still has some disadvantages, such as high cost, limited cobalt resources, toxicity, etc.

Therefore, the recycling of spent $LiCoO_2$ electrodes has many advantages such as an alternative cobalt resource, mitigation of environmental pollution, etc. The data from London Metal Exchange from January to October 2004 showed that the price of cobalt is about two times more expensive than nickel, 24 times more expensive than aluminum, and 15 times more expensive than copper [5]. As a result, it is necessary to recycle the $LiCoO_2$-based Li-ion batteries. The recovered cobalt may be used to make either alloys with magnetic properties or new electrodes [6–9].

As potential predominant magnetic and electrical resistive materials, cobalt ferrite nanoparticles with a ferrimagnetic cubic spinel structure are characterized as an important class of soft magnetic materials, have large magneto crystalline anisotropy and reasonable magnetization, and are widely used in many electronic and magnetic applications, such as high-density magnetic recording media, high-performance electromagnetic and spintronic devices, ferrofluids, magnetic resonance imaging, etc. [10–12]. Owing to their excellent magnetic, luminescent, and mechanical properties, various methods to prepare cobalt ferrite nanoparticles with high-electromagnetic performance have been reported, including coprecipitation, spray drying, freeze drying, sol–gel, self-propagating combustion and hydrothermal methods [13–18]. Among these methods, more and more attention has been paid to sol–gel and self-propagating combustion methods [19, 20]. The advantages of the sol–gel method are relatively low preparation temperature and high reactive activity, leading to as-synthesized materials with homogeneity and accurate stoichiometric composition. The characteristics of the self-propagating combustion method are to use the internal chemical energy of raw materials to complete the synthesis. The advantages of this method are simple process, low energy loss, high production yield and high product purity. At the same time, numerous studies have been reported on recycling spent Li-ion batteries. However, there was no report on preparation of ferrimagnetic cobalt ferrite nanoparticles by using spent Li-ion mobile phones batteries. In this study, the authors have reported a novel way to recycle spent Li-ion batteries by combining the chemical sol–gel process with the combustion process and the target products are not a single metal or its oxide but ferrimagnetic cobalt ferrite nanoparticles with high value.

Experimental

Chemical composition of Li-ion batteries

A Li-ion battery consists of a plastic casing and several cell units. Each cell unit has a cathode, an anode, an organic separator, an organic electrolyte, and a Ni-coated steel casing. Table 1 shows a typical chemical composition of the Li-ion batteries [4].

Raw materials

Two spent Li-ion mobile phone batteries (manufactured 2000) were employed in this study. Li-ion batteries were manually dismantled and physically separated into their different parts: anode, cathode, steel, separators, and current collectors. Cathodic active materials from spent Li-ion batteries were separated by a series of thermal treatment, high-speed shredding, calcination steps [4].

Synthesis of $Co_{0.8}Fe_{2.2}O_4$ nanoparticles

The cathodic active materials obtained as raw materials to prepare nanocrystalline cobalt ferrites were dissolved in 4 mol L^{-1} HNO_3 containing 2.5 wt% H_2O_2. The mixed solution was stirred continuously at 353 K for 2 h. After complete dissolution, the mixed solution was filtered in order to obtain the pure cobaltous hydroxide precipitate and avoid the production of impurities in the final product, and an orange yellow clear solution was obtained. Then, an aqueous solution of 40 wt% NaOH was used as the precipitating agent. The pH value of the mixed solution was constantly monitored while the NaOH solution was added. The mixed solution was constantly stirred using a magnetic stirrer until the pH level of 9.0–10 during the coprecipitation process. To isolate the supernatant liquid, the mixed solution was centrifuged for 15 min at 2,500 rpm, and the cobaltous hydroxide precipitate was obtained. The supernatant liquid was then decanted and cobaltous nitrate and ferric nitrate solution was obtained by dissolving the cobaltous hydroxide sedimentation in 2 mol L^{-1} HNO_3 containing 2.5 wt% H_2O_2. After that, the concentrations of Co^{2+} and Fe^{3+} were analyzed by inductively coupled plasma (ICP). In order to prepare cobalt ferrite ($Co_{0.8}Fe_{2.2}O_4$) nanoparticles [21], 0.05 L of 0.02 mol L^{-1} cobaltous nitrate and ferric nitrate solution was obtained by adding suitable amounts of analytical grade $Co(NO_3)_2$ and $Fe(NO_3)_2$ to adjust the concentrations of Co^{2+} and Fe^{3+}. Furthermore, an appropriate amount of citric acid was put into the solution to adjust the molar ratio of the total concentrations of metal ions to citric acid, leading to 1.0:0.75. Following the adjustment of a pH level of 7.0 by aqua ammonia, during this procedure, the

Table 1 Average chemical composition of Li-ion batteries

Component	$LiCoO_2$	Steel/Ni	Cu/Al
Wt%	27.5	24.5	14.5
Component	Carbon	Electrolyte	Polymer
Wt%	16	3.5	14

solution was continuously stirred by a magnetic agitator, and the temperature was controlled at 348 K, until the solution became saturated and formed the brown–red sol. The sol was put into a dish and dried in an oven at 408 K for 8 h, and then transformed into dried gels. Igniting the dried gels, a self-propagating combustion process occurred and the dried gels after combustion was obtained. Finally, The cobalt ferrite ($Co_{0.8}Fe_{2.2}O_4$) nanoparticles were prepared via calcining the dried gels after combustion at 1173 K for 2 h. The experiments were run in triplicate, and errors for each experiment were always below 3%.

Analytical methods

The thermal properties of the products were carried out by thermogravimetric analysis (TG) and differential thermal analysis (DTA) (model DT-40, Japan) at a heating rate of 283 K/min in static air. Infrared spectrum (IR) (model TENSOR-27, Germany) of the samples was measured by a spectrophotometer from 400 to 4000 cm^{-1} using the KBr pellet method. The phase identification of the dried gels before combustion and after combustion, and the dried gels after combustion calcined at 1173 K for 2 h were performed by X-ray diffraction (XRD) (model BRUKER.axs, Germany) with Cu K_α radiation. The microstructure of cobalt ferrite was observed using transmission electron microscopy (TEM) (model JEM-100SK, Japan). Stoichiometry analysis of the cobalt ferrite ($Co_{0.8}Fe_{2.2}O_4$) nanoparticles was carried out by inductively coupled plasma (ICP) (model Optima 2100DV, America).

Results and discussion

Self-propagating combustion process of the dried gels

The autocatalytic nature of the combustion process of the dried gels was investigated by TG–DTA measurements and the results are presented in Fig. 1. The experimental DTA curve shows obviously two exothermic peaks. It can be seen that the first exothermic peak at around 462.3 K is relatively sharp and intense, and the related TG curve shows large weight loss near this temperature. The result is attributed to the decomposition of the dried gels occurring in a single step, which is induced by autocatalytic oxidation–reduction reaction between the nitrate and the citrate acid. The second exothermic peak at around 585.8 K is relatively wide as well, but the related TG curve shows only a small weight loss near this temperature, which is contributed to the decomposition of the rest of the organic matter.

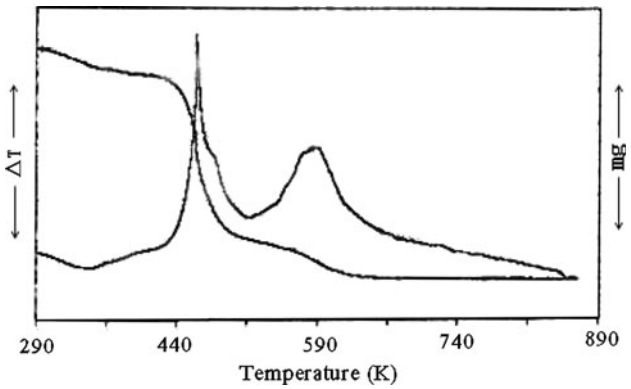

Fig. 1 TG and DTA curves of the dried gels powder

IR spectrum of the dried gels before combustion and after combustion

The information on the chemical changes taking place during the combustion process could be obtained by infrared spectra analysis, which would be very helpful for understanding combustion-related reaction mechanism. Figure 2 shows the IR spectrums of the dried gels before combustion and after combustion at different molar ratio of the total concentration of metal ions to citric acid at a pH level of 7.0 within the range of 400–4000 cm^{-1}. Data analysis on the IR spectrum of the dried gels before combustion indicates that the characteristic bands peaking at 3300–2500 and 1600 cm^{-1} originate from the stretching vibration of the O–H group and the antisymmetric stretching vibration of the carboxyl group in Fig. 2a. In addition, the characteristic band of NO_3^- ion is also shown at about 1450–1300 and 830–800 cm^{-1}, respectively. Which indicates that the NO_3^- group existed in the structure of citrate gels during the process of gelation. After the combustion process, the strength of the IR absorption bands corresponding to O–H group, carboxyl group and NO_3^- disappeared completely. These variations reflected by the IR spectra before and after burning indicate that both the carboxyl group and NO_3^- took part in the reaction during combustion process. Furthermore, a new absorption band peaking at 571 cm^{-1} appears. It can be seen from Fig. 2c, d that there is only one obvious band at about 571 cm^{-1}, which is identified to correspond to the characteristic band of M–O(M = Fe, Co) stretching vibration mode. Therefore, the combustion occurred here could be considered as a thermally induced anionic redox reaction process of the xerogel, in which the carboxyl groups act as a reductant while NO_3^- ions act as an oxidant. Because the nitrate ions provide an in situ oxidizing environment for the decomposition of the organic component, the oxidation reaction is highly accelerated and finally leads to a self-propagating combustion process of nitrate–citrate gel. Which could be explained as follows, with the amount of

aqua ammonia addition and the solution continuously stirring the following reaction occurs:

$$C_6H_8O_7(aq) + Co^{2+} + Fe^{3+} + NO_3^- + NH_3 \cdot H_2O(aq) \rightarrow Co_{0.8}Fe_{2.2}O_4(aq) + CO_2(g) + NH_3(g) + NO_2(g) + H_2O(g)$$

Comparing Fig. 2b with c and d, the cobalt ferrite nanoparticles could be formed during combustion with the molar ratio (1:0.75 or 1:1) of the total concentration of metal ions to citric acid because of a new absorption band peaking at 571 cm^{-1} appears, and the characteristic band of NO_3^- ion at about 1450–1300 cm^{-1} disappeared completely.

IR spectrum of the dried gels after combustion calcined at 1173 K for 2 h

Figure 3 shows that the IR spectrums of the dried gels after combustion at 1173 K for 2 h at different molar ratio of the total concentration of metal ions to citric acid at a pH of 7.0 within the range of 400–4000 cm^{-1}. The characteristic band of cobalt ferrite nanoparticles at about 571 cm^{-1} could be obviously found in Fig. 3. By comparing Fig. 3b with a and c, the strongest IR absorption bands is in Fig. 3b, Its IR absorption bands intensity between Fig. 3a and c. Therefore, the cobalt ferrite nanoparticles could be formed during the dried gel after combustion calcined at 1173 K for 2 h with the molar ratio (1.0:0.75) of the total concentration of metal ions to citric acid.

XRD patterns of the dried gels before combustion and after combustion calcined at 1173 K for 2 h

Generally, XRD can be used to characterize the crystallinity of nanoparticles, and it gives average diameters of all the nanoparticles. The precipitated fine particles were

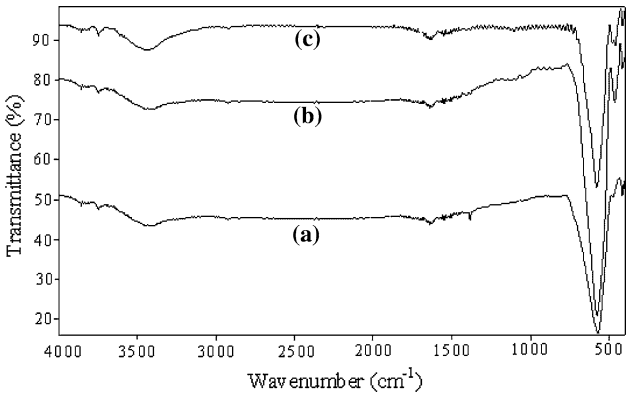

Fig. 3 IR spectrums of the dried gel after combustion calcined at 900 °C for 2 h on different molar ratio (*a*) 1.0:0.5, (*b*) 1.0:0.75, (*c*) 1:1

characterized by XRD for structural determination and estimation of crystallite size. XRD patterns were analyzed and indexed using powder X software [22]. For monitoring the phase evolution of the dried gels before combustion and after combustion, XRD experiments were carried out in Fig. 4, Fig. 4a shows the XRD of the dried gels before combustion are amorphous naturally, but the XRD of the dried gels after combustion calcined at 1173 K for 2 h is a ferrimagnetic cobalt ferrite nanoparticles with a cubic spinel structure in Fig. 4b–d. The strongest reflection comes from the (3 1 1) plane, which denotes the spinel phase. The peaks indexed to (2 2 0), (3 1 1), (2 2 2), (4 2 2), (5 1 1), and (4 4 0) planes of a cubic unit cell, correspond to cubic spinel structure. The crystallite size of the powder is estimated from the X-ray peak broadening of the (3 1 1) diffraction peak Fig. 4c using Scherrer equation:

$$t = \frac{0.9\,\lambda}{\sqrt{\left(B_M^2 - B_S^2\right)}\cos\theta}$$

t means the crystallite size, B_M is the full width at half maximum of the sample, and B_S is that of a standard

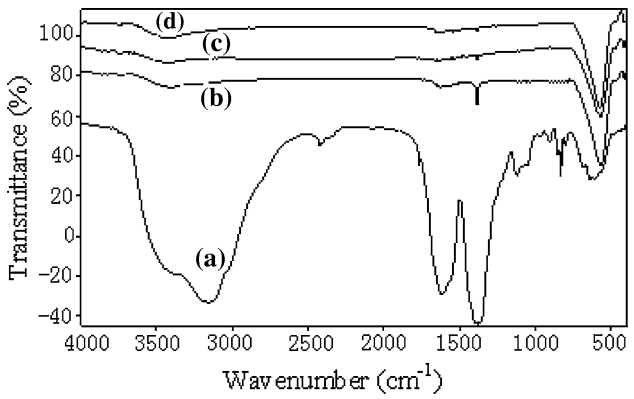

Fig. 2 IR spectrums of the dried gels before combustion (*a*) and after combustion on different molar ratio (*b*) 1.0:0.5, (*c*) 1.0:0.75, (*d*) 1:1

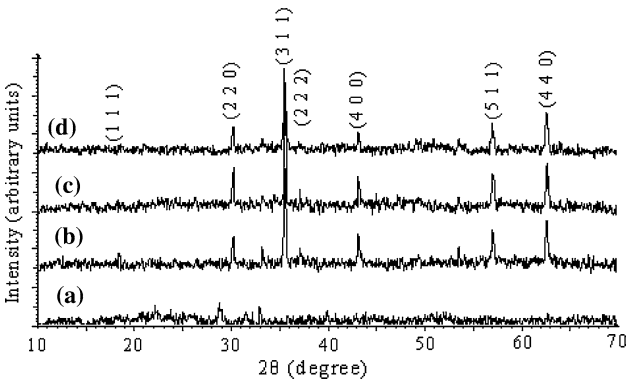

Fig. 4 XRD patterns of the dried gels before combustion (*a*) 1:0.75 and after combustion calcined at 900 °C for 2 h (*b*) 1:0.5, (*c*) 1:0.75, (*d*) 1:1

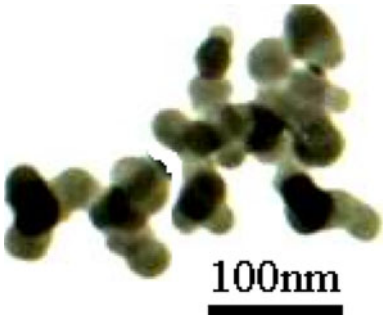

Fig. 5 TEM photograph of the dried gels after combustion calcined at 900 °C for 2 h

crystallite size of around 2 μm. λ is the X-ray wave length and θ is the angle of diffraction. The mean crystallite size estimated from the (3 1 1) peak is approximately 23.5 nm.

TEM photograph of the dried gels after combustion calcined at 1173 K for 2 h

The TEM photograph of the dried gels after combustion is shown in Fig. 5. The particle size of ferrimagnetic cobalt ferrite estimated from the photograph is below 25 nm and the morphology of the particles is almost spherical. The TEM photograph is also shown that the cobalt ferrite nanoparticles synthesized with the combination of the sol–gel and the dried gels after combustion calcined at 1173 K for 2 h methods were well-dispersed and with little aggregation.

Stoichiometry analysis of the dried gels after combustion calcined at 1173 K for 2 h

A 0.30 g powder of the dried gels after combustion calcined at 1173 K for 2 h was dissolved in HNO_3. After digestion, the solution was evaporated to dryness; the residue was transferred into a volumetric flask and made up to the 0.025 L with ultrapure water. Blank solutions were prepared in the same way as the samples. The precise metal ion stoichiometry of Co and Fe was measured by inductively coupled plasma (ICP), the results showed 26.60 and 69.73 wt%, respectively. The result is almost equal to the initial stoichiometry ($Co_{0.8}Fe_{2.2}O_4$) in the solution after adjusting the metal ion.

Conclusions

The ferrimagnetic cubic spinel cobalt ferrite nanoparticles with an average crystallite size of 23.5 nm could be prepared with the combination of the sol–gel and the dried gels after combustion calcined at 1173 K for 2 h methods using the spent lithium batteries as raw materials, which provides an alternative way to recycle spent Li-ion batteries.

The dried gels reaction products exhibited auto-combustion behavior at room temperature, the essence of the auto-combustion process of dried gels could be considered as a thermal-induced autocatalytic anionic redox reaction. In the redox reaction, nitrate ion played an important role in providing the oxidizing environment, lowering the decomposition temperature of the organic component, and increasing the rate of the oxidation reaction, which could result in a self-propagating combustion.

References

1. Ra D, Hana KS (2006) J Power Sources 163:284
2. Sheem KY, Sung M, Lee YH (2010) Electr Acta 55:5808
3. Xu J, Thomas HR, Francis Rob W, Lum Ken R (2008) J Power Sources 177:512
4. Lee CK, Rhee KI (2003) Hydrometallurgy 68:5
5. Mantuano DP, Dorella G, Elias RCA, Mansur MB (2006) J Power Sources 159:1510
6. Freitas MBJG, Garcia EM, Celante VG (2009) J Appl Electrochem 39:601
7. Li J, Zhao R, He XM, Liu HC (2009) Ionics 15:111
8. Fang G, Qian N (2011) Adv Mater Res 183–185:1553
9. Jyoko Y, Kashiwabara S, Hayashi Y (1997) J Electrochem Soc 144:L5
10. Nana F, Nobuki T, Satoshi S (2010) J Jap Ins Metals 74:345
11. Gul IH, Maqsood A, Naeem M, Naeem Ashiq M (2010) J Alloys Compd 507:201
12. Arulmurugan R, Vaidyanathan G, Sendhilnathan S, Jeyadevan B (2005) Phys B 368:223
13. El-Shobaky GA, Turky AM, Mostafa NY, Mohamed SK (2010) J Alloys Compd 493:415
14. Vaidyanathan Sendhilnathan GS, Arulmurugan R (2007) J Magn Magn Mater 313:293
15. Toksha BG, Shirsath Sagar E, Patange SM, Jadhav KM (2008) Solid State Commun 147:479
16. Zhao L, Zhang H, Xing Y, Song S, Yu S, Shi W, Guo X, Yang J, Lei Y, Cao F (2008) J Solid State Chem 181:245
17. Gul IH, Abbasi AZ, Amin F, Anis-ur-Rehman M, Maqsood A (2008) J Magn Magn Mater 320:270
18. Suwalka O, Sharma RK, Sebastian V, Lakshmi N, Venugopalan K (2007) J Magn Magn Mater 313:198
19. Yousefi MH, Manouchehri S, Arab A, Mozaffari M, Amiri Gh R, Amighian J (2010) Mater Res Bull 45:1792
20. Xiao S, Jiang W, Li L, Li X (2007) Mater Chem Phys 106:82
21. Zi ZF, Zhang SB, Wang B, Zhu XB, Yang ZR, Dai JM, Song WH, Sun YP (2010) J Magn Magn Mater 322:148
22. Dong C (1999) J Appl Crystallogr 32:838